Skimming impacts and rebounds of arbitrarily shaped bodies on shallow liquid layers

Ryan Palmer, Frank Smith

Department of Mathematics,
University College London (UCL), London
e-mail: ryan.palmer.14@ucl.ac.uk

BAMC 2019 - University of Bath

Coupled fluid-body motion for a **skimming impact of an arbitrarily shaped solid body on a shallow liquid layer**.

The body shape is **parametrized by its typical scaled curvature** C for which rebound dynamics are predicted.

- **Two geometrical scenarios** are of interest: $C < 0$ producing a hooked body and $C > 0$ producing a rounded underside.
- **Reduced analysis and physical insights** are made in each case alongside numerical investigations.
- **Analyses of small-time water entry and of water exit solutions** are described and shown to be in close agreement with the numerical predictions.

- Ducks and drakes/skimming stones

- Aircraft icing.
  Wing photo from Aviation Education Multimedia Library.
  Ice crystal photo from Lawson et al. (2006)

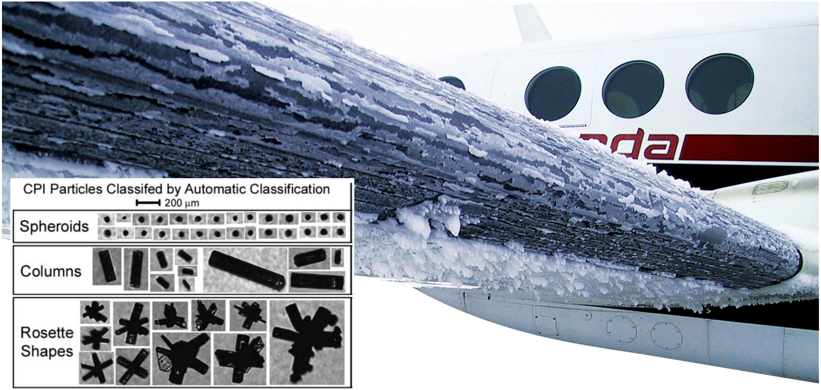

The main assumptions made in the theory include:

- the two-dimensionality of the entire fluid-body interaction,
- the neglect of air effects,
- the incompressibility of the quasi-inviscid fluid (water),
- the shallowness of the water layer,
- the smallness of the flow angles induced during the motion.

Scales:

- liquid layer depth is small compared to particle length,
- horizontal velocity large compared to vertical,
- body thickness is thinner than the water layer.

Background equations

The shallow-water equations (i.e. unsteady inviscid boundary-layer equations) nominally apply to the fluid flow *in this scenario due to the large Reynolds number, Froude number and Weber number. Hence, at leading order the effects of viscosity, gravity and surface tension are negligible.*

In a frame of reference centred on the body, in non-dimensional form **the model gives a horizontal velocity, the body half-length and a typical convective time of** $O(1)$.

Of primary interest in the analysis of this system is the wetted region $[x_1, x_0]$**.**

Background equations

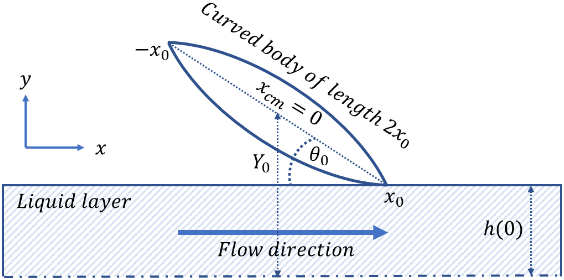

h: liquid layer thickness;
u: horizontal flow velocity;
p: fluid pressure;
Y: vertical position of the body's centre of mass;
θ: inclination of the body to the flow;
T: body-shape function.

$$(h, u, p, Y, \theta, T) = (1, 1, 0, 1, 0, 0) + \left(\tilde{h}, \tilde{u}, \tilde{p}, \tilde{Y}, \tilde{\theta}, \tilde{T}\right) + \ldots , \quad (1)$$

Background equations

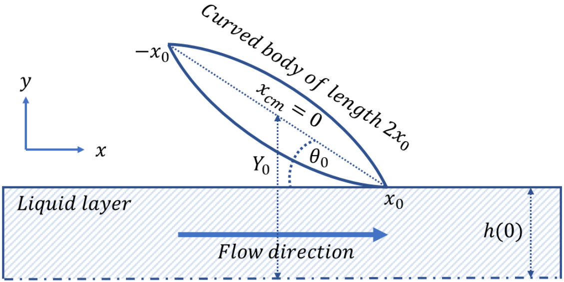

The trailing edge is considered to be sharp with the liquid free surface detaching there. For a body of arbitrary scaled geometry $\tilde{T}(x)$ the free surface height under the body, within the wetted region, is given by:

$$\tilde{h}(x,t) = \tilde{Y}(t) + (x - x_{cm})\tilde{\theta}(t) - \tilde{T}(x). \tag{2}$$

Since the flow is irrotational, the pertubations provide the shallow-water equations:

$$\tilde{u}_t + \tilde{u}_x = -\tilde{p}_x \qquad x_1 \leq x \leq x_0, \tag{3a}$$

$$\tilde{h}_t + \tilde{h}_x + \tilde{u}_x = 0 \qquad x_1 \leq x \leq x_0. \tag{3b}$$

At the unknown leading edge $x_1 = x_1(t) \in [-x_0, x_0]$ - typically $O(1)$, jump condition are found as in Hicks and Smith (2010), Tuck and Dixon (1989):

$$\tilde{p}(x_1, t) + \left(1 - x_1'\right) \tilde{u}(x_1, t) = 0, \tag{4}$$

with

$$\tilde{u}(x_1, t) = -\left(1 - x_1'\right) \tilde{h}(x_1, t). \tag{5}$$

The vertical momentum equation for the body is:

$$M\tilde{Y}'' = \int_{x_1}^{x_0} \tilde{p}(x,t)dx, \tag{6}$$

where M is the scaled mass of the body.

The angular-momentum equation of the body is:

$$I\tilde{\theta}'' = \int_{x_1}^{x_0} (x - x_{cm})\tilde{p}(x,t)dx. \tag{7}$$

where I is the scaled moment of inertia for the body.

Of primary interest in the analysis of this system is the wetted region $[x_1, x_0]$. Additionally, the responses of Y, V, θ, ω and P are to be evaluated.

System of equations

The body shape is described by an arbitrary polynomial $T(x)$ of order n defined across the body's length $x \in [-x_0, x_0]$.

The only limitation is that $T(x_0) = 0 = T(-x_0)$ and x_0 and $-x_0$ should be simple roots. Thus:

$$T(x) = (x_0 - x)\left(\sum_{m=0}^{n-1} a_m x^m\right), \qquad \sum_{m=0}^{n-1} a_m(-x_0)^m = 0. \tag{8}$$

Given the definition of the body geometry, (3a) and (3b) imply that p_{xx} is at most order x^{n-2} for $n > 2$ and linear in x for $n \leq 2$.

The pressure response can be written as:

$$p = \begin{cases} \sum_{m=0}^{n} \gamma_m x^m, & n > 2. \\ \sum_{m=0}^{3} \gamma_m x^m, & n \leq 2. \end{cases} \tag{9}$$

The coefficients $\gamma_m, \; m = 0, 1, ..., n$ are unknown functions of time.

System of equations

This system of equations can be used to model the body trajectory:

$$Y' = V, \tag{10}$$

$$\theta' = \omega, \tag{11}$$

$$V' = \sum_{m=0}^{n} \frac{\gamma_m}{M(m+1)} \left(x_0^{m+1} - x_1^{m+1} \right), \tag{12}$$

$$\omega' = \sum_{m=0}^{n} \frac{\gamma_m}{I(m+2)} \left(x_0^{m+2} - x_1^{m+2} \right), \tag{13}$$

$$D' = V + \theta - \gamma_1 - a_1 x_0 + a_0, \tag{14}$$

$$x_1' = 1 - \left[\frac{\sum_{m=0}^{n} \gamma_m x_1^m}{Y + x_1\theta - (x_0 - x_1)\left(\sum_{m=0}^{n-1} a_m x_1^m\right)} \right]^{1/2}. \tag{15}$$

System of equations

Additionally:

$$\sum_{m=0}^{n} \gamma_m x_1^m = \frac{\left[D - \frac{1}{2}\omega x_1^2 - x_1\left(Y' + \theta\right) + \sum_{m=0}^{n-1}(x_0 a_{m+1} - a_m)x_1^{m+1}\right]^2}{Y + x_1\theta - (x_0 - x_1)\left(\sum_{m=0}^{n-1} a_m x_1^m\right)}. \tag{16}$$

$$\gamma_2 - \omega - (a_1 - x_0 a_2) = \sum_{m=0}^{n} \frac{\gamma_m}{2M(m+1)}\left(x_0^{m+1} - x_1^{m+1}\right). \tag{17}$$

$$\gamma_3 - (a_2 - x_0 a_3) = \sum_{m=0}^{n} \frac{\gamma_m}{6I(m+2)}\left(x_0^{m+2} - x_1^{m+2}\right). \tag{18}$$

$$\sum_{m=0}^{n} \gamma_m x_0^m = 0. \tag{19}$$

$$\gamma_m = (a_{m-1} - x_0 a_m), \text{ for } m > 3. \tag{20}$$

Small-time entry solution

Small-time solutions for the particle's entry into the water layer are used to initialise the computational results.

The configuration of the plate upon impact is known so that asymptotic expansions can be produced for Y, θ, x_1, D and $\gamma_m, \ m = 0, 1, 2, ...n$.

Working through we obtain two constraints:

- $Y_0 + x_0\theta_0 = 0$ giving a geometric constraint for the body entering an initially undisturbed water layer,
- $D_0 = x_0^2\omega_0/2 + x_0(V_0 + \theta_0 + a_0)$ giving a relation between the initial fluid velocity and the body's initial configuration.

Small-time entry solution

$$\hat{x}_1 = \frac{-3(x_0\omega_0 + V_0) - \sqrt{9(x_0\omega_0 + V_0)^2 + 8\left(\theta_0 + \sum_{m=0}^{n-1} a_m x_0^m\right)(x_0\omega_0 + V_0)}}{4\left(\theta_0 + \sum_{m=0}^{n-1} a_m x_0^m\right)}. \tag{21}$$

A key difference: takes into account the tangential angle of the body geometry at the trailing edge.

If the x_0 root in $T(x)$ had a multiplicity $k > 1$ the small time solution for $\hat{x}_1$ follows that of a straight plate, since the $\hat{x}_1 \sum_{m=0}^{n-1} a_m x_0^m$ term becomes $\hat{x}_1^k t^k \sum_{m=0}^{n-k} a_m x_0^m$.

Exit solution

The exit solution and behaviour for γ_0, γ_1, x_1 and the leading edge pressure found for a straight plate still holds in the general case:

- unbounded response in γ_0 and γ_1,
- $\gamma_m, m = 2, 3, ..., n$ remain bounded throughout.
- $(x_1 - x_0)(\sum_{a=0}^{n-1} a_m x_1^m)$ is negligible as exit is approached.

The same analytical approach and arguments are thus valid for the general polynomial case. That is:

$$p_1 = \frac{Y_0 + x_0\theta_0}{\log(\alpha(t_e - t))^2} + ... ,$$

indicating that a rapid change in pressure is expected towards water exit.

Effect of large camber

To analyse how the body's rebound behaviour may be affected by large positive or negative camber, suppose that:

$$a_m = \hat{a}_m C, \qquad m = 0, 1, 2, ..., n; \qquad \hat{a}_m > 0; \qquad \hat{a}_m \sim O(1)$$

with C taken to be large, consider the negative case.

Substituting (16) into (15), the evolution of x_1 is governed by:

$$x_1' = 1 - \frac{\left[-D + \frac{1}{2}\omega x_1^2 + x_1 \left(V + \theta\right) - \sum_{m=1}^{n} (x_0 a_m - a_{m-1}) x_1^m\right]}{Y + x_1\theta - (x_0 - x_1)\left(\sum_{m=0}^{n-1} a_m x_1^m\right)}. \tag{22}$$

Effect of large camber

$$x_1' = 1 - \frac{-\left(D + \sum_{m=1}^{n} x_0 a_m x_1^m\right) + \frac{1}{2}\omega x_1^2 + x_1 V + x_1\left(\theta + \sum_{m=0}^{n} a_m x_1^m\right)}{\left(Y - x_0 \sum_{m=0}^{n-1} a_m x_1^m\right) + x_1\left(\theta + \sum_{m=0}^{n-1} a_m x_1^m\right)}. \quad (23)$$

$D_0 = \frac{1}{2}\omega x_1^2 + x_0(v_0 + \theta_0 + a_0) \Rightarrow D \approx x_0 a_0 \sim O(C)$. As $\mid C \mid \to \infty$:

$$x_1' \to 1 - \frac{-\sum_{m=0}^{n} x_0 a_m x_1^m + x_1 \sum_{m=0}^{n} a_m x_1^m}{-\sum_{m=0}^{n-1} x_0 a_m x_1^m + x_1 \sum_{m=0}^{n-1} a_m x_1^m} \to 0. \quad (24)$$

Hence, the wetted region of the body tends to some constant as the derivative of $x_1 \to 0$. In particular, from (21), as $\mid C \mid \to \infty$:

$$\hat{x}_1 \to \frac{-\sqrt{-8\left(\theta_0 + \sum_{m=0}^{n-1} a_m x_0^m\right)}}{4\left(\theta_0 + \sum_{m=0}^{n-1} a_m x_0^m\right)} \to 0. \quad (25)$$

Downward hooked body

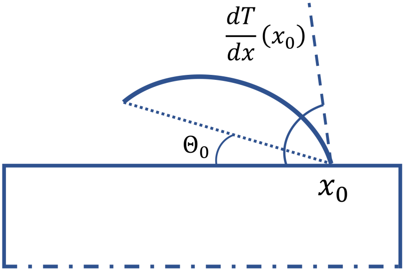

Figure: *Geometric configuration for* $T(x) = C(x_0 - x)(x_0 + x), C < 0$. *Here* θ_0 *refers to the angle made between the water surface and a straight line that connects the body's ends.*

Unless otherwise stated, the initial conditions used for each case are: $Y_0 = 20, V_0 = -1, \theta_0 = -20, \omega_0 = 0$ with $D_0 = x_0^2\omega_0/2 + x_0(V_0 + \theta_0 + a_0)$ and $M = 2, I = 1$.

Downward hooked body

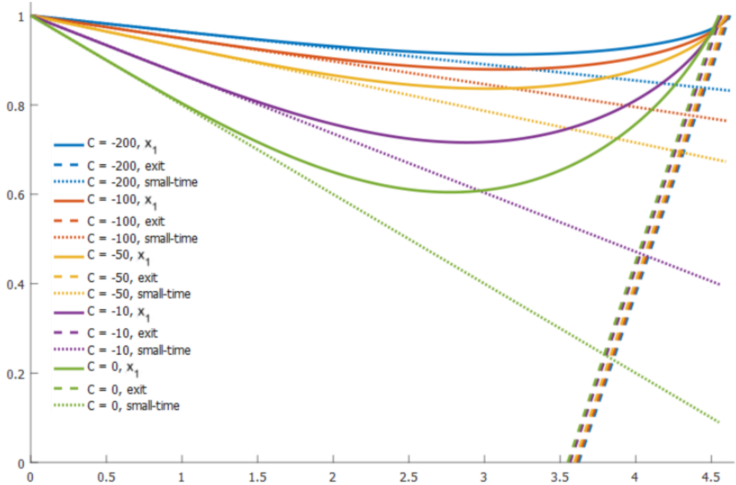

Figure: $C < 0$ - *Evolution of the leading-edge position x_1 as a function of time for varying C.*

Downward hooked body

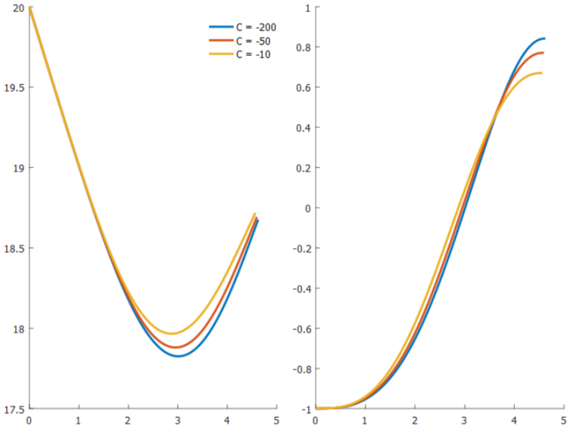

Figure: $C < 0$ - *Left: Evolution of the vertical position of the body's centre of mass, Y, as a function of time for varying C. Right: Evolution of the vertical velocity of the body, V, as a function of time for varying C.*

Downward hooked body

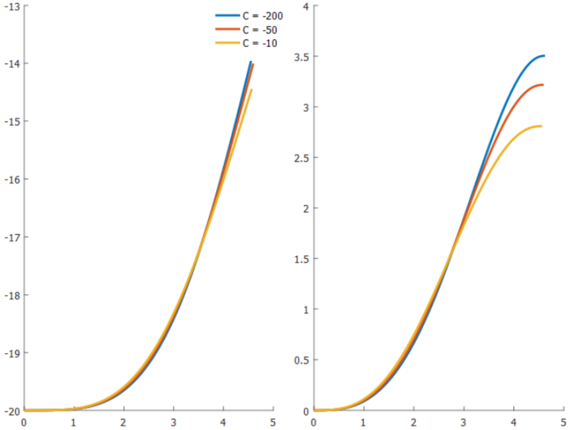

Figure: $C < 0$ - *Left: Evolution of the body's angle, θ, as a function of time for varying C. Right: Evolution of the angular velocity of the body, ω, as a function of time for varying C.*

Downward hooked body

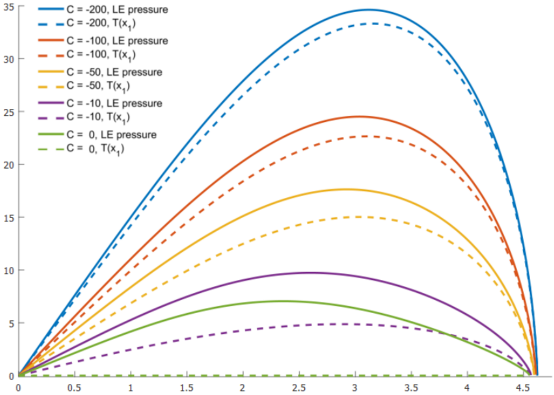

Figure: $C < 0$ - *Evolution of the leading edge pressure on the body as a function of time for varying* C. *The corresponding body thickness at* x_1 *is shown for comparison.*

For any point, $x \in [x_1, x_0]$, as $\mid C \mid \rightarrow \infty$, $Y, Y', \theta, \theta', D, D'$ are all $O(1)$, and only $a_m \sim O(C)$, $m = 0, 1, 2, ..., n$, so that the pressure approximates to:

$$p(x) = \sum_{m=0}^{n} \gamma_m x^m = \left(-D' + Y' + \theta\right)\left(x - x_0\right) + \left(\frac{Y''}{2} + \theta'\right)\left(x^2 - x_0^2\right)$$

$$+ \left(\frac{\theta''}{6}\right)\left(x^3 - x_0^3\right) + \sum_{m=1}^{n}\left(a_{m-1} - x_0 a_m\right)\left(x^m - x_0^m\right),$$

$$\rightarrow -\left(x - x_0\right)\left(\sum_{m=0}^{n-1} a_m x^m\right) = -T(x).$$

This result holds for all body shapes of a downward hook geometry.

The wetted region remains small for large curvature, $x_1 \sim x_0$, then $\sum_{m=0}^{n-1} a_m x_1^m \sim \sum_{m=0}^{n-1} a_m x_0^m$, the derivative of $T(x)$ at x_0.

$$x_1' \approx 1 - \frac{-\left(D + \sum_{m=0}^{n-1} x_0 a_m x_0^m - x_0 a_0\right) + \frac{1}{2}\omega x_1^2 + x_1 Y' + x_1\left(\theta + \sum_{m=0}^{n} a_m x_0^m\right)}{\left(Y - x_0 \sum_{m=0}^{n-1} a_m x_0^m\right) + x_1\left(\theta + \sum_{m=0}^{n-1} a_m x_0^m\right)}. \tag{26}$$

Define:

$$\bar{D} = D + \frac{dT}{dx}(x_0) - x_0 a_0, \qquad \bar{\theta} = \theta + \frac{dT}{dx}(x_0)$$

$$\bar{Y} = Y - x_0 \frac{dT}{dx}(x_0), \qquad x_1' \approx 1 - \frac{-\bar{D} + \frac{1}{2}\bar{\theta}' x_1^2 + x_1 \bar{Y}' + x_1 \bar{\theta}}{\bar{Y} + x_1 \bar{\theta}}.$$

The trailing edge of any concave shaped body may be approximated by a straight plate at an increased initial angle θ_0.

Downward hooked body

By such an analogy **the system of equations can be reduced** and used to model either a **steep flat plate or a downward hooked particle** of large camber.

Consider a straight plate at a high angle equivalent to large $C < 0$. Then:

$$\theta \sim O(C); \;\; Y \sim O(C); \;\; D \sim O(C).$$

All other parameters are $O(1)$ throughout.

Notably, D', γ_0 and γ_1 blow up near exit time; however, since this is over a short time scale, they are treated as $O(1)$.

Downward hooked body

At leading order:

$$\hat{\gamma}_0 = -\hat{\theta} x_0; \qquad \hat{\gamma}_1 = \hat{\theta}; \qquad \hat{\gamma}_m = 0, m = 2, 3, ..., n,$$

$$\hat{x}_1' = 1 - \left[\frac{\hat{\theta}(\hat{x}_1 - x_0)}{\hat{Y} + \hat{x}_1 \hat{\theta}} \right]^{1/2}.$$

Motion only depends on the angle and height of centre of mass:

$$M\hat{Y}'' = \hat{\theta} \left(\frac{x_0^2 - \hat{x}_1^2}{2} - (x_0 - \hat{x}_1) \right), \; I\hat{\theta}'' = \hat{\theta} \left(\frac{x_0^3 - \hat{x}_1^3}{3} - \frac{x_0^2 - \hat{x}_1^2}{2} \right).$$

The pressure across the wetted region becomes:

$$p(x) = \hat{\theta}(\hat{x} - x_0).$$

Finally, $\hat{\theta}$ grows negatively large, the small-time solution becomes:

$$\hat{\hat{x}}_1 = -\frac{\sqrt{-2\hat{\theta}_0}}{2\hat{\theta}_0}.$$

Downward hooked body

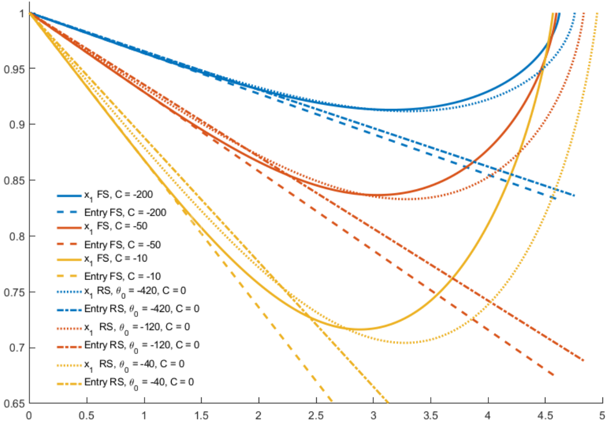

Figure: *Evolution of the leading-edge position x_1 as a function of time for $C = -200, -50$ and -10 for the full system and reduced system with $\tilde{\theta}_0 = -420, -120$ and -40 respectively.*

Downward hooked body

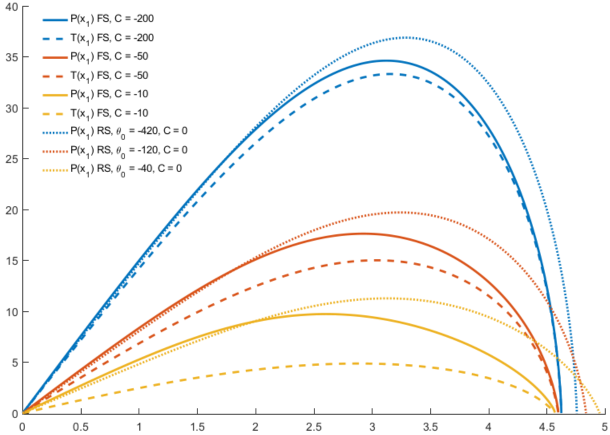

Figure: *Evolution of the leading-edge pressure as a function of time for* $C = -200, -50$ *and* -10 *for the full system and reduced system with* $\tilde{\theta}_0 = -420, -120$ *and* -40 *respectively.*

Downward hooked body

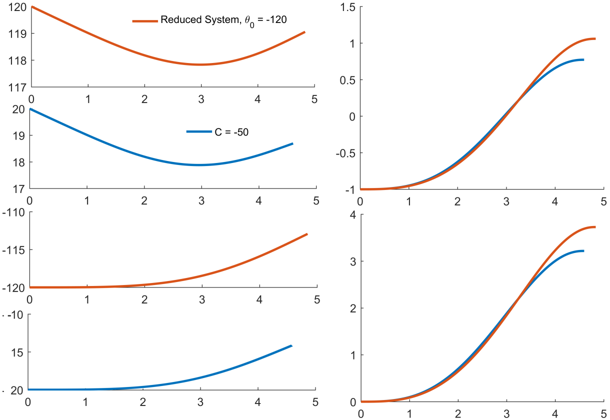

Figure: *Evolution of (Top left) Y, (Top right) V, (Bottom left) θ and (Bottom right) ω as a function of time for the full system with $C = -50$ and reduced system with $\tilde{\theta}_0 = -120$.*

Curved underside body - fixed body angle

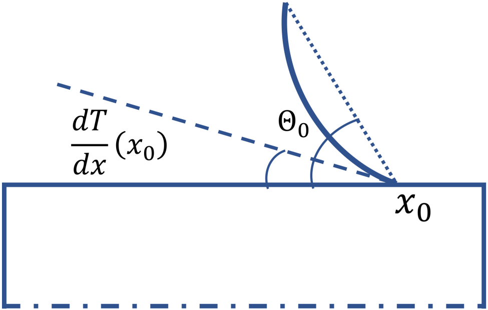

Figure: Geometric configuration for $T(x) = C(x_0 - x)(x_0 + x)$, $C > 0$. Here θ_0 refers to the angle made between the water surface and a straight line that connects the body's maxima. For increasing C, the effective body angle $\hat{\theta}_0 = \theta_0 - T_x(x_0)$ decreases.

Curved underside body - fixed body angle

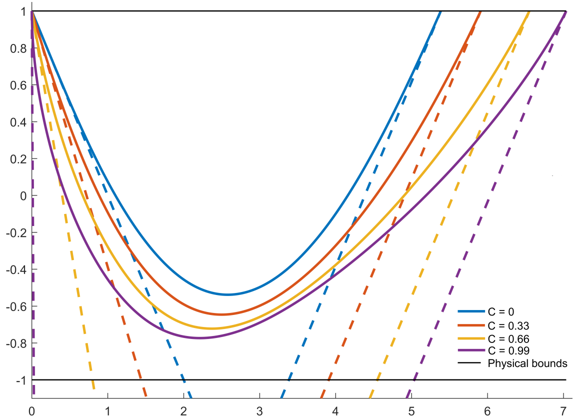

Figure: *Evolution of the leading-edge position x_1 as a function of time for fixed body angle $\theta_0 = -2$ and $C = 0, 0.33, 0.66$ and 0.99. The linear asymptotic behaviour at small-time and for exit are also shown.*

Curved underside body - fixed body angle

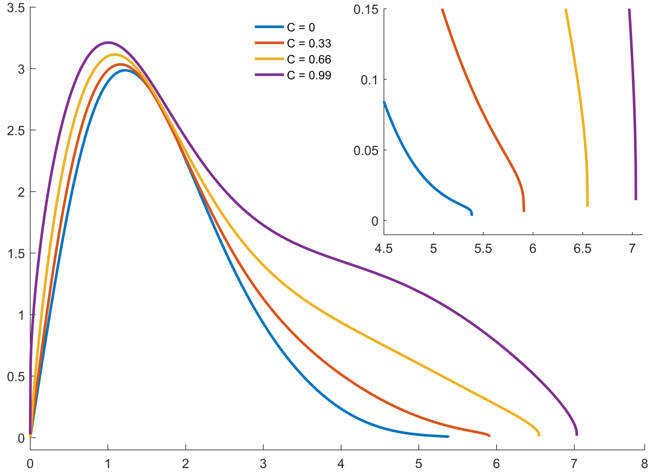

Figure: *Evolution of the leading-edge pressure as a function of time for fixed body angle* $\theta_0 = -2$ *and* $C = 0, 0.33, 0.66$ *and* 0.99.

Curved underside body - fixed body angle

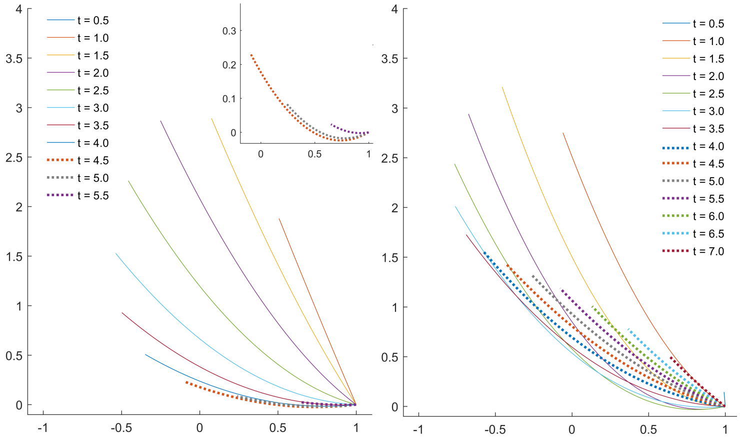

Figure: *Evolution of the underbody pressure at several time intervals for fixed body angle* $\theta_0 = -2$ *and* $C = 0$ *and* $C = 0.99$.

Curved underside body - fixed body angle

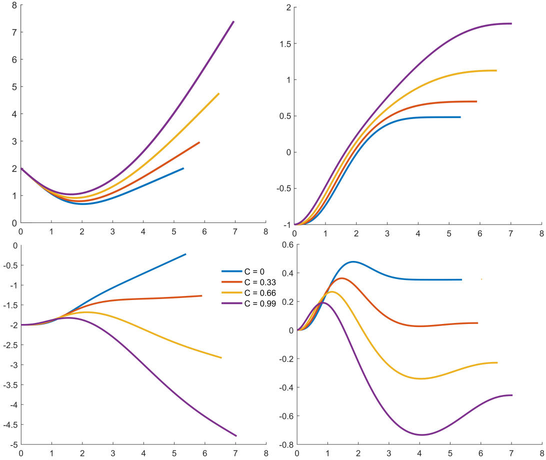

Figure: *Evolution of (Top left) Y, (Top right) V, (Bottom left) θ and (Bottom right) ω as a function of time.*

Conclusions

Previous models have been **extended** to explain the interaction between a **rigid body, of arbitrary shape undergoing a skimming impact** on a shallow liquid layer.

- **For a hooked particle** a significant rotation occurs causing the particle to leave the liquid layer at a smaller height than that at which it entered.
- **For a curved underside with fixed body angle** a super-elastic response occurs with increased curvature.

Reduced order systems of ODEs for the skimming motion have been derived and shown to be in close agreement .

Limitation:

- Concave case, setting the initial angle at too shallow of a pitch leads to cavitation.

Future work:

- Allow for the trailing edge to move freely by incorporating an additional momentum jump condition at the trailing edge.
- This allows solutions with splash jets both in front and behind the body, as in Howson et al. (2004).
- Incorporation of gravity effects for larger bodies or the consideration of a series of impacts for variously shaped particles.

Acknowledgements

We gratefully acknowledge discussions with and interest from Richard Moser, Ian Roberts and Colin Hatch, all of AeroTex UK, and from Robert Bowles, Nick Ovenden, Sergei Timoshin, Samire Balta. We further recognise the support of this work from EPSRC through grants EP/R511638/1, GR/T11364/01, EP/G501831/1, EP/H501665/1, EP/K032208/1 during part of this research and from UCL (IAA award) and AeroTex.

References

[1] Photo by the Aviation Education Multimedia Library : https://aeml.tech.purdue.edu/

[2] Lawson, R. P., Baker, B., Pilson, B. and Mo, Q., 2006. In Situ Observations of the Microphysical Properties of Wave, Cirrus, and Anvil Clouds. Part II: Cirrus Clouds, Journal of the Atmospheric Sciences, 63(12), pp.3186-3203.

[3] Hicks, P.D. and Smith, F.T., 2010. Skimming impacts and rebounds on shallow liquid layers. Proceedings of the Royal Society A: Mathematical, Physical and Engineering Sciences, 467(2127), pp.653-674.

[4] Liu, K. and Smith, F.T., 2014. Collisions, rebounds and skimming. Philosophical Transactions of the Royal Society A: Mathematical, Physical and Engineering Sciences, 372(2020), p.20130351.

[5] Tuck, E.O. and Dixon, A., 1989. Surf-skimmer planing hydrodynamics. Journal of Fluid Mechanics, 205, pp.581-592.

[6] Howison, S.D., Ockendon, J.R. and Oliver, J.M., 2004. Oblique slamming, planing and skimming. Journal of engineering mathematics, 48(3-4), pp.321-337.

Thank you for your attention.

Are there any questions?